International Journal of Automation and Control

ISSN online: 1740-7524 - ISSN print: 1740-7516
https://www.inderscience.com/ijaac

Error-based ADRC approach of lower knee exoskeleton system for rehabilitation

Nasir Ahmed Alawad, Amjad Jaleel Humaidi, Ahmed Sabah Al-Araji

DOI: 10.1504/IJAAC.2025.10061844

Article History:

Received:	09 August 2023
Last revised:	14 December 2023
Accepted:	16 December 2023
Published online:	02 December 2024

Error-based ADRC approach of lower knee exoskeleton system for rehabilitation

Nasir Ahmed Alawad*

Faculty of Engineering,
Department of Computer Engineering,
Mustansiriyah University,
BP, 10052, Iraq
Email: cse.20.33@grad.uotechnology.edu.iq
*Corresponding author

Amjad Jaleel Humaidi

Department of Control and System Engineering,
University of Technology,
BP, 10066, Iraq
Email: amjad.j.humaidi@uotechnology.edu.iq

Ahmed Sabah Al-Araji

Department of Computer Engineering,
University of Technology,
BP, 10066, Iraq
Email: ahmed.s.alaraji@uotechnology.edu.iq

Abstract: In this study, active disturbance rejection control (ADRC) has been designed to control the exoskeleton system for rehabilitation at knee level and to replace the exercises made by physicians with systematic training devices. The time derivative of reference input and feed-back signals is an evitable in most ADRC schemes. To alleviate the burden due to derivative actions, the idea of proposing error-based ADRC (EADRC) has been introduced. In a conventional ADRC scheme, the extended state observer (ESO) is the core element of the controller to estimate both the states of the system and the exerted disturbance. The EADRC utilises the estimates in the error sense rather than the actual states. The EADRC technique is compared to traditional ADRC and the numerical results showed that the proposed EADRC outperforms the conventional ADRC in terms of tracking errors, noise and load rejection capabilities for the system subjected to noise and load uncertainties.

Keywords: exoskeleton system; ADRC; active disturbance rejection control; robustness; stability; knee rehabilitation.

Reference to this paper should be made as follows: Alawad, N.A., Humaidi, A.J. and Al-Araji, A.S. (2025) 'Error-based ADRC approach of lower knee exoskeleton system for rehabilitation', *Int. J. Automation and Control*, Vol. 19, No. 1, pp.1–17.

Biographical notes: Nasir Ahmed Alawad received his BSc in Control and System Engineering from University of Technology, Iraq, in 1981, MSc in Control and Instrumentation Engineering from University of Technology, Iraq in 1984. He is presently Prof. in Computer Engineering Department, Al-Mustansiriyah University, Iraq. His fields of interest include control theory, computer control and computer aided design of control.

Amjad Jaleel Humaidi received his BSc and MSc in Control Engineering from Al-Rasheed College of Engineering and Science, University of Technology, Baghdad, Iraq, in 1992 and 1997, respectively. He received his PhD from University of Technology in 2006 with specialisation of control and automation. He is presently a Staff Member in Control and Systems Engineering Department. His fields of interest include adaptive control, nonlinear control, nonlinear observers, intelligent control, optimisation, identification and real-time image processing.

Ahmed Sabah Al-Araji had finished BSc in Control and Systems Engineering from the University of Technology in 1997 and MSc in Mechatronics Engineering for the University of Technology in 2001. He has finished his PhD in Electronics and Computer Engineering in the School of Engineering and Design, Brunel University, London, UK in 2012. He is presently Head-Assistant of Computer Department at the University of Technology.

1 Introduction

According to Han (2008), Humaidi and Badr (2018a, 2018b), Abdul-Adheem et al. (2021), the fundamental idea behind active disturbance rejection control (ADRC) is to represent a system's uncertainty, modelling error, as well as outside influences as an extended state, including actual estimation and adjustment provided by the extended state observer (ESO). Motion control (Tian and Gao, 2009; Zhao and Gao, 2010), chemical process control (Zheng et al., 2009), micro-electro-mechanical systems (MEMS) control (Zheng et al., 2007), exoskeleton design control of the lower knee(Nasir et al., 2023a), linear systems with interval time-varying state-delay (Venkatesh et al., 2021) and hybrid power system (Vivek et al., 2023) have all used ESO and ADRC as a new, developing control design tool to handle many sorts of control challenges across several engineering disciplines. Several literature, particularly technical problems (Gernot, 2013; Song et al., 2019; Congzhi et al., 2020), can get into considerable detail on this topic. The reference signal and its derivatives are considered to be known prior to control design in traditional ADRC (CADRC) designs. However, because there is a decision loop beyond the low-level control loop that calculates the reference signal quickly, in many actual systems, only the reference signal at the current moment is available. An error-based ADRC design is presented and successfully implemented in a DC–DC buck converter as a result of this challenge (Madonski et al., 2019a). Furthermore, the literature (Madonski et al., 2019b) reveals that error-based ADRC is capable of addressing harmonic disturbances effectively. The present stability study for error-based ADRC, on the other hand, is dependent on the premise that the initial estimation error is sufficiently modest

(Madonski et al., 2019a), which may not be met in practice. Establishing a strong stability theory for error-based ADRC is essential. Additionally, developing a much more appropriate error-based ADRC for multidisciplinary approach is a significant issue. The ADRC method depends on a recovery loop that enables parameter variations disturbances in the input signal path to be rejected. This produces in a feedback linearised system in terms of an *n*th order integrator chain, where *n* is the system's relative degree. As a result, using direct and active estimation and rejection converts the system to a linear one, which can be solved using a simple control problem solution (Dariusz et al., 2020). A proposal to construct the ADRC controller in an error domain (today termed as the EADRC), which allows the calculation of reference trajectory derivatives to be avoided, has also been given, independently in both (Michael, 2016) and more frequently in(Ramirez-Neria et al., 2020).

The following list highlights the paper's significant contribution:

a Most ADRC approaches in use today express themselves in 2DOF output-based form. This imposes restrictions on the conventional ADRC. Because of this, a comparison between the recently proposed 1DOF error-based formulation of ADRC and the traditional 2DOF output-based ADRC is done in this work.

b Another useful benefit of expressing the ADRC in error-based form is that it can be used for trajectory tracking when reference time derivatives are not available.

c The controlled system's stability and global convergence properties have been demonstrated and satisfied by using Lyapunov stability method.

The paper's remaining sections are organised as follows. Knee-Joint modelling is discussed in Section 2. In Section 3, controllers based on ADRC and EADRC are presented and evaluated. Section 4 presents the stability analysis, the simulation results and a discussion is showed in Section 5, while Section 6 gives the conclusion of the work.

2 Knee-joint mathematical model

The knee is a pivot joint for relative mobility between the upper and lower halves of the limb. Inside the sagittal plane, it gives one degree of freedom in flexion and extension movement. Human-Exoskeleton System In a planar sitting position, a lower limb exoskeleton enables knee flexion and extension, as depicted in Figure 1. A simple equation for the motion of a human lower limb attached to a knee joint exoskeleton during routine activities is given by (Nasir et al., 2023a; Christopher et al., 2021; Saber and Djamel, 2019). Simultaneously, kinetic modelling of the biological limb and exoskeleton is developed. It is represented by the associated system's Lagrangian L_a:

$$L_{ai} = E_{ki} - E_{gi} \tag{1}$$

E_{ki}, E_{gi} represents, the system's component's respective kinematic and gravity energies, and (i = 1, 2) with a person's limb and exoskeleton.

$$E_{ki} = \frac{1}{2} J_i \dot{\theta}^2 \tag{2}$$

where J_i the inertia of the human leg and exoskeleton, $\dot{\theta}$ is acceleration of the coupled system.

$$E_{gi} = m_i g l_i \left(1 - \sin\theta\right) \tag{3}$$

m_i is the mass of the human leg and exoskeleton, g is the acceleration due to gravity, l_i is the distance between the knee joint and centre of gravity, while θ is knee-joint angle. The system dynamics after deriving L_a can be expressed as:

$$J_i\ddot{\theta} = m_i g l_i \cos\theta - \tau_{exti} \tag{4}$$

where τ_{exti} represents the external torque applied to the system.

$$\tau_{exti} = \tau_{fi} + \tau_e \tag{5}$$

τ_{fi} and τ_e are the friction and exoskeleton control torques respectively, with:

$$\tau_{fi} = -A_i sign\dot{\theta} - B_i\dot{\theta} \tag{6}$$

A_i and B_i are the solid and viscous friction coefficients respectively.

The system model for the exoskeleton and human leg can be obtained by:

$$J\ddot{\theta} = -\tau_g cos\theta - A_i sign\dot{\theta} - B_i\dot{\theta} + \tau_e + \tau_h \tag{7}$$

where J, τ_g, τ_e, τ_h are Inertia, gravity torque, controller torque and human torques (uncertainty and external disturbances) respectively and:

$$J = \sum_{i=1}^{2} J_i, \tau_g = \sum_{i=1}^{2} \tau_{gi}, A = \sum_{i=1}^{2} A_i \ , B = \sum_{i=1}^{2} B_i$$

Leg flexion as well as extension movements are considered synchronised and continuous since the exoskeleton and the user's joints are safely coupled in the model. Rehabilitation robots act as assistive device to therapists and give new chances for improving the rehabilitation process, according to some study. Furthermore, robots can save therapists time by removing the need for time-consuming supervision of repetitious and progressive exercise (Gallagher et al., 2022).

Figure 1 Schematic human-exoskeleton system

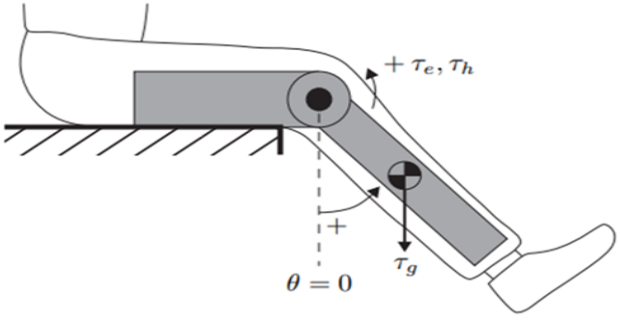

We investigated a sinusoidal shape of the knee joint angle path with magnitude for the desired motion patterns of (0.785 rad) for extension motion and (−0.785 rad) for flexion motion this is defined by:

$$r = 0.785.\sin\left(2.\pi\ .1.57t\right)$$

It is required to control the inserted exoskeleton torque (τ_e) for D.C motor to move the lower leg in a described path (r) in a short time (settling time) and without vibration (stable system). The exoskeleton was powered by a brushless DC motor. This makes it appropriate for use in practical cases.

3 EADRC methodology

Return to equation (7), and Letting x_1 and x_2 represent the variables θ and $\dot{\theta}$. This equation can be written in state variable as:

$$\begin{aligned} \dot{x}_1 &= x_2 \\ \dot{x}_2 &= f + b\tau \end{aligned} \tag{8}$$

where $b = 1/J$ and f represents the lumped term of uncertainties and nonlinearities, which is given by:

$$\frac{1}{J}\left[\tau_g \cos\left(x_1\right) - f_v x_2 - f_s sign\left(x_2\right) + \tau_h\right]$$

Because the system is second order, an extra state should be introduced to the ADRC control to eliminate the aggregated component of uncertainty and nonlinearities (Gao, 2014). Rather than the conventional output-based approach of determining state variables as $x = \left[x_1 x_2 x_3\right] = \left[y\ \dot{y}\ f\right]$, where $y = \theta, \dot{y} = \dot{\theta}$ as found in standard ADRC designs for second order plant models, the state variables are determined by examining the tracking error(e) description:

$$\begin{aligned} e &= r - y = x_1 \\ \dot{e} &= \dot{r} - \dot{y} = \dot{x}_1 = x_2 \\ \ddot{e} &= \ddot{r} - \ddot{y} = \ddot{x}_1 = \dot{x}_2 = \ddot{r} - f - bu = x_3 - bu \\ \text{Let } x_3 &= f^* = \ddot{r} - f \end{aligned} \tag{9}$$

The purpose is to select a set of phase state variables that will allow the otherwise inaccessible term ($\ddot{r}$) to be included in the extended state variable, and therefore treated as part of the total disturbance ($x_3 = f^*$), which will be calculated and compensated in the disturbance rejection loop. The goal now is to stabilise the new output signal (e) at zero with the same control input (u), besides the effect of total disturbances (f^*) by modifying the control problem in error-based form (Dariusz et al., 2020; Radosiaw and Dariusz, 2021). Equation (8) can be written in alternative coordinates:

$x = \left[x_1 x_2 x_3\right] = \left[e\ \dot{e}\ f^*\right]$ or virtually extended form as:

$$\begin{cases} \dot{x}_1 = x_2 \\ \dot{x}_2 = x_3 - bu \\ \dot{x}_3 = \dot{f}^* \end{cases} \tag{10}$$

For the considered plant model can be proposed as:

$$\begin{cases} \dot{z}_1 = z_2 + \beta_1 \varepsilon \\ \dot{z}_2 = z_3 - bu + \beta_2 \varepsilon \\ \dot{z}_3 = \beta_3 \varepsilon \end{cases} \quad \text{The aim is} \rightarrow \begin{cases} z_1 \rightarrow x_1 \\ z_2 \rightarrow x_2 \\ z_3 \rightarrow x_3 \end{cases} \tag{11}$$

where $z = [z_1\, z_2\, z_3] = [\hat{x}_1\ \hat{x}_2\ \hat{x}_3]$ the vector of state variables is estimates, and $\varepsilon \cong e - z_1$ is the observer estimation error. The fundamental goal of this extended-state-observer (ESO) is to recover data more about active total disturbance ($z_3 \rightarrow f^*$) in a quick and accurate way, which is required for its cancellations. The following formula can be used to calculate the observer gain matrix:

$$\boldsymbol{\beta} = \begin{bmatrix} 3\omega_o & 3\omega_o^2 & \omega_o^3 \end{bmatrix} \tag{12}$$

The bandwidth ω_o of an (ESO) all that is required to identify the constituents of an observer gain matrix. This easy tuning strategy, on the other hand, integrates the performance and noise sensitivity trade-offs (Chen et al., 2011). Whereas the system's control law (u) of the system. Equation (9) can be calculated as follows:

$$u = \frac{u_0 + f^*}{b} = \frac{k_p z_1 + k_d z_2 + z_3}{b} \text{ or } u = \frac{k_p (r - y) + k_d (\dot{r} - \dot{y}) + z_3}{b} \tag{13}$$

The aforementioned control actions can be viewed of as variations on traditional output-based ADRC with extra feed-forward, but with the undetermined terms estimated through by the observer. Here the linear controller, which represent the proportional-derivative (PD), Where (k_p) is proportional and (k_d) is derivative gains, in this work can be chosen as $k_p = \omega_c^2$, $k_d = 2\omega_c$ .Where (ω_c) is the control loop bandwidth. If one chooses the bandwidth of observer to be $\omega_o = 4\omega_c$, then it easy to calculate the elements of observer matrix gains (β_1 , β_2 , β_3) according to equation (12) and the values of controller gains (Nasir et al., 2023a).

Substituting equation (13) into equation (11) we have:

$$\begin{cases} \dot{z}_1 = z_2 + \beta_1 (e - z_1) = -\beta_1 z_1 + z_2 + \beta_1 e \\ \dot{z}_2 = z_3 - (k_p z_1 + k_d z_2 + z_3) + \beta_2 (e - z_1) \\ \dot{z}_3 = \beta_3 (e - z_1) = -\beta_3 z_1 + \beta_3 e \end{cases} \tag{14}$$

Rewritten equation (14) in the state space form we have:

$$\dot{z} = A_e z + \beta e, \text{ where } z = \begin{bmatrix} z_1 \\ z_2 \\ z_3 \end{bmatrix}$$

$$A_e = \begin{bmatrix} -\beta_1 & 1 & 0 \\ -\beta_2 - k_p & -k_d & 0 \\ -\beta_3 & 0 & 0 \end{bmatrix}, \tag{15}$$

$$\beta = \begin{bmatrix} \beta_1 \\ \beta_2 \\ \beta_3 \end{bmatrix}$$

When compared the matrix (A_e) in equation (15) with original matrix in conventional ADRC, where:

$$A_c = \begin{bmatrix} -\beta_1 & 1 & 0 \\ -\beta_2 & 0 & 1 \\ -\beta_3 & 0 & 0 \end{bmatrix}$$

The change was only detected in the second row of both matrices (A_e, A_c). The feed-forward element is properly considered as significant distinction between ADRC and EADRC. Obviously, the feed-forward element is completely approximated in the EADRC structure, on other hand both traditional ADRC and EADRC control techniques are shown in Figure 2. In conventional ADRC, one of its inputs is the system output signal $y(t)$ and the second input is the control signal $u(t)$, while, in EADRC one of its inputs is the feedback error signal (t) and the second input is the control signal $u(t)$. It should be highlighted, however, that the robustness, flexibility, and ability of the traditional ADRC have not been compromised by the EADRC, which simplifies control synthesis and parameter adjustments. It also removed the common need for higher-order derivatives to be available, making the need for additional sensors or differentiators unnecessary.

Figure 2 Shows two ADRC approaches: (a) conventional ADRC and (b) EADRC

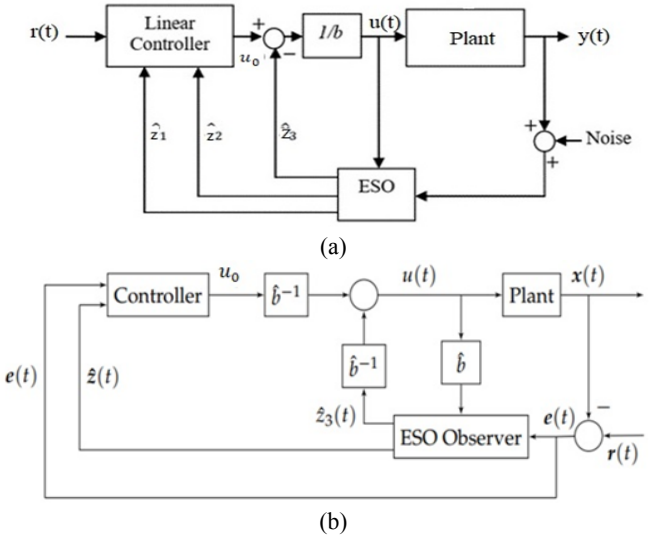

4 System stability analysis

Assume that the goal of the control design is to force the output of the plant to correspond a certain bounded reference signal r and its derivatives, $\dot{r},\ddot{r},\ldots,r^n$ which are all bounded. In most cases, when a closed-loop control system is linear, the stability may be quickly examined by calculating out the control system's Eigen values. The stable nature of the control system is indicated by all of the Eigen values with negative real parts. Based on the Lyapunov second methodology, the stabilities of the linear ESO and the ADRC system were examined. The following was demonstrated:

1 Appropriate observer gains exist, this means the estimation errors between the ESO and system states are convergent; and

2 Appropriate gains of the linear controller (PD) exist, and the ADRC system is stable, i.e., the estimation errors between the transient profiles and the system outputs are convergent.

Theorem 1: *Assuming equation (15) is Hurwitz and it is always possible to select* $\beta_1,\beta_1,\beta_1,k_p,k_d$ *in such a way that the eigenvalues of* A_e *are in the left-hand of s-plane.*

Proof. Since A_e is Hurwitz, there exists a unique positive definite matrix *P* such that:

$$A_e^T P + PA_e = -Q \tag{16}$$

For any given positive definite matrix *Q*. The Lyapunov theory states that (e) should go closer to zero as time approaches infinity in order for the estimated error to asymptotically converge. Defining a Lyapunov function,

$$V(t) = z^T Pz \tag{17}$$

The time derivative of equation (17) is giving by:

$$\dot{V}(t) = \dot{z}^T Pz + z^T P\dot{z} \tag{18}$$

by substituting equation (15) into equation (18), it can be obtained:

$$\dot{V}(t) = \left(A_e z + \beta\right)^T Pz + z^T P\left(A_e z + \beta\right) = z^T A_e^T Pz + z^T PA_e z + 2\beta^T Pz \tag{19}$$

by substituting equation (16) into equation (19), it can be obtained:

$$\begin{aligned} &\dot{V}(t) = -z^T Qz + 2\beta^T Pz \\ &\dot{V}(t) \le -\delta Q \,\|\, z \,\|^2 + 2\varepsilon \,\|\, P \,\|\,\|\, z \,\| \end{aligned} \tag{20}$$

After a sufficiently long time, the norm of the state error z is bounded by:

$$\|\, z \,\| \le \frac{2\varepsilon \,\|\, P \,\|}{\delta Q} \tag{21}$$

where δ is the smallest eigenvalue of a matrix A_e. The Lyapunov stability theory demonstrates that the system is in uniform stability, where $V(t) > 0$ and $\dot{V}(t) < 0$. All

signals in the aforementioned equations, including the tracking error $e(t)$ and its differential $\dot{e}(t)$, are bounded. The proof has been completed.

5 Computer simulation and discussion

In this section, we compare two control methods that were introduced in Section 3. The goal of this study was to determine which strategy provides a favourable response and effectively counteracts the effects of disturbances. This study used a 33-year-old healthy male who weighs 75 kilos and measures 1.73 m tall. The tested system, as shown in Figure 1, consists of a human in a sitting position wearing a lower limb exoskeleton, as well as parameters based on Table 1 for this scenario (Saber and Djamel, 2019).Integral of the absolute magnitude of error (IAE), integral square error (ISE), Integral square of the control signal (ISU), integral absolute of the control signal (IAU), and Root Mean Square Error (RMSE) are some of the performance indicators used to analyse tracking accuracy (Domingos et al., 2021; Wameedh et al., 2020; Nasir et al., 2023b).

Table 1 Numeric values of system parameters

Parameter	*Value*
Inertia (J)	0.348 kg. m^2
Solid friction coefficient (f_s)	0.998 N.m
Viscous friction coefficient (f_s)	0.872 N.m.s./rad
Gravity torque (τ_g)	3.445 N.m

To validate the effectiveness of the proposed control strategy (EADRC) for rehabilitation system, computer simulations were run in the Matlab/Simulink environment. Assume that the observers and controller gains were the same in both techniques. Allow for a settling time of 0.4 s and w_c = 24.5 rad/s in the design.

Case 1 with constant disturbance

The first simulation is carried out with a constant disturbance of 0.5 N.m. at time t = 2 sec to evaluate the performance of the EADRC controller with payload condition. Figure 3 depicts the EADRC and CADRC's performance (Desired vs. Real output). For both EADRC and CADRC, Figure 4 shows the difference in knee position between the desired and actual positions. The ADRC without feed-forward has a substantially slower transient response, as seen in figure, in addition, as shown in Table 2, comparison experiment results indicate that the EADRC control approach achieves the minimum tracking error, demonstrating its effectiveness and superiority to CADRC. Because it is not provided with any new information that could potentially divest the ESO, it was assumed that CADRC without feed forward would have the weakest effectiveness of the evaluated scenarios. In this case, settling time refers to the amount of time that occurs between applying the disturbance and the controller's ability to return the trajectory to the desired input. It was clear that the EADRC controller reduced overshot, which shortened the amount of time needed to reach the predetermined settling time. In contrast to ADRC,

which has a higher overshot and needs more time. Figure 5 depicts the control efforts required to study the required control torque (τ_e) or $u(t)$ for both control systems. When compared to the EADRC control technique, comparative experiment results indicate that the CADRC control method produces the shortest control effort required for a controller (ISU) and the smallest measure of chattering reduction in control signal index (IAU). This is because the CADRC response torque denies the perturbation quickly.

Table 2 Performance indices for EADRC and CADRC with constant disturbance

Control method	*RMSE* (rad.)	*IAE* (rad.)	*ISE* (rad.)	*ISU* (N.m)	*IAU* (N.m)
CADRC	0.0747	0.1377	0.0289	220.1	41.39
EADRC	0.0539	0.0402	0.0087	1400	77.78

Figure 3 Time response comparison between EADRC and CADRC with constant disturbance (see online version for colours)

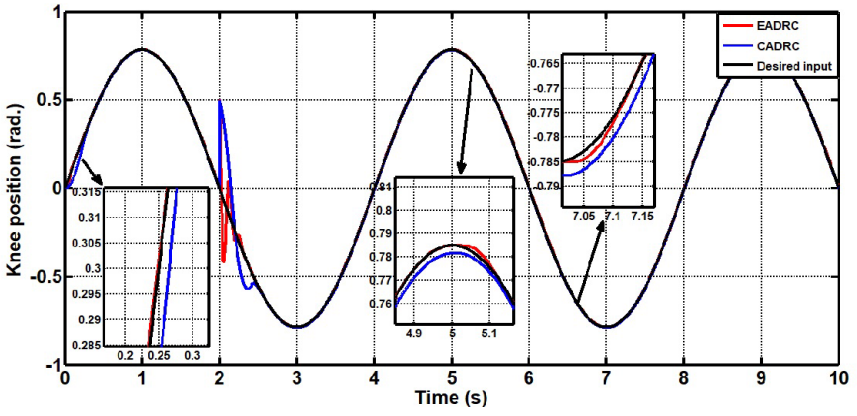

Figure 4 Tracking error comparison between EADRC and CADRC with constant disturbance (see online version for colours)

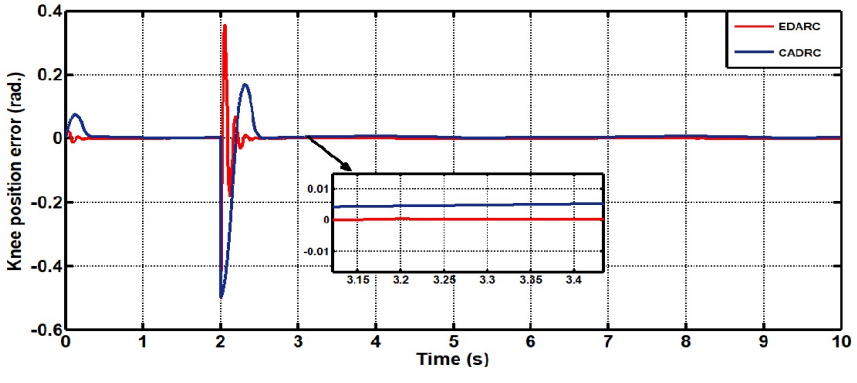

We plot extra state $Z_3(t)$ vs. its aim to assess the ESO's performance (total disturbances). Disturbances are depicted in Figure 6. For EADRC, estimate $Z_3(t)$ shows a strong correlation with total disturbances.

Figure 5 Control torque required for comparison between EADRC and CADRC with constant disturbance (see online version for colours)

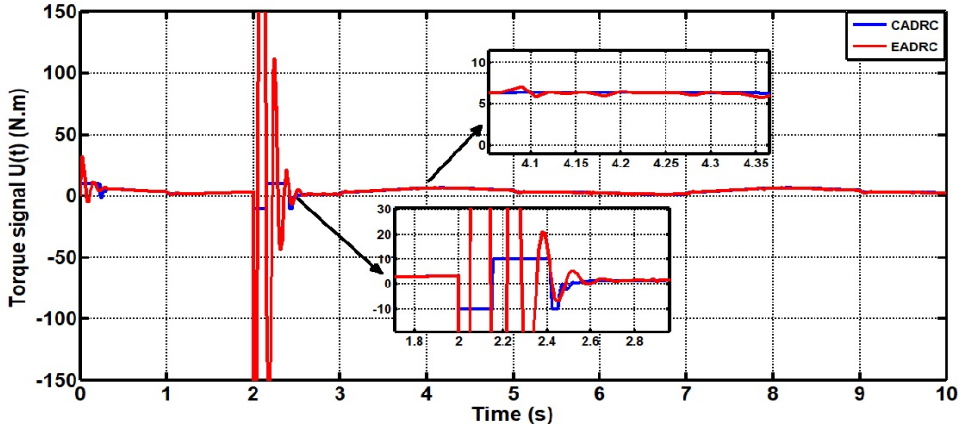

Figure 6 Total disturbances and its estimation for EDRC with constant disturbance (see online version for colours)

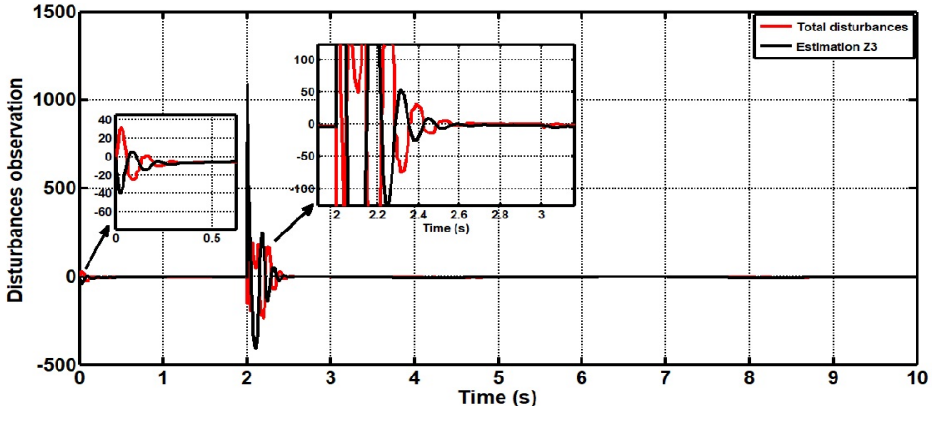

Case 2 with noise disturbance

It should be viewed as an important foundation because technological activity comprises of various mechanical and electrical components that are all impacted by external noise. Consider the case of Gaussian noise with (0.0001) variation and a mean value of (0). The trajectory tracking performance is shown in Figure 7; all position responses appear to follow the expected trajectory, even with minimal vibration, particularly at the EADRC response. The discrepancy in knee angles between the desired and actual positions is depicted in Figure 8. In comparable studies, the EADRC control technique achieves the lowest tracking error, confirming its utility and superiority. Figure 9 depicts the control efforts required to study the required control torque (τ_e) or $u(t)$ for both control systems. When compared to CADRC, the EADRC control method yields the shortest control effort required for a controller (ISU) and the smallest measure of chattering reduction in control signal index (IAU), as shown in Table 3.

Table 3 Performance indices for EADRC and CADRC with noise disturbance

Control method	*RMSE* (rad.)	*IAE* (rad.)	*ISE* (rad.)	*ISU* (N.m)	*IAU* (N.m)
CADRC	0.0118	0.0743	0.00138	580.4	68.18
EADRC	0.0038	0.0279	0.00013	341.7	47.42

Figure 7 Time response comparison between EADRC and CADRC with noise disturbance (see online version for colours)

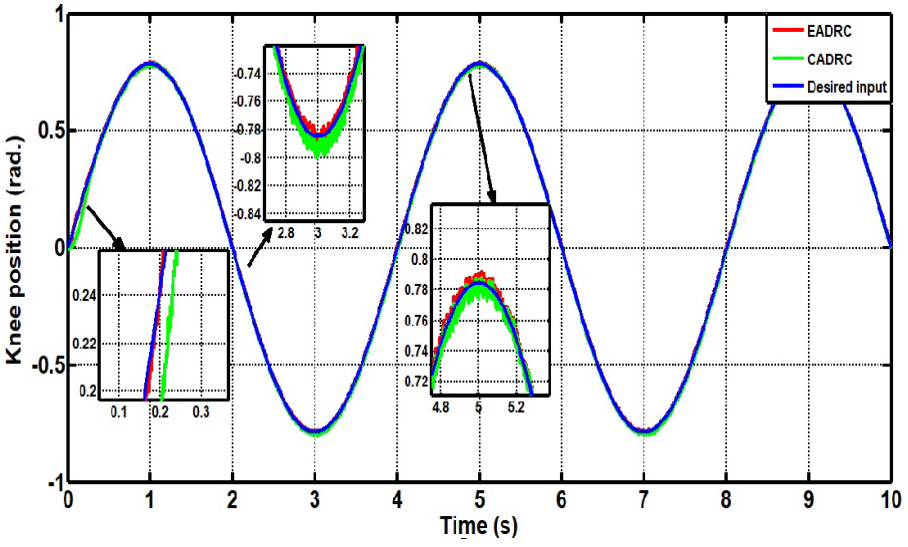

Figure 8 Tracking error comparison between EADRC and CADRC with noise disturbance (see online version for colours)

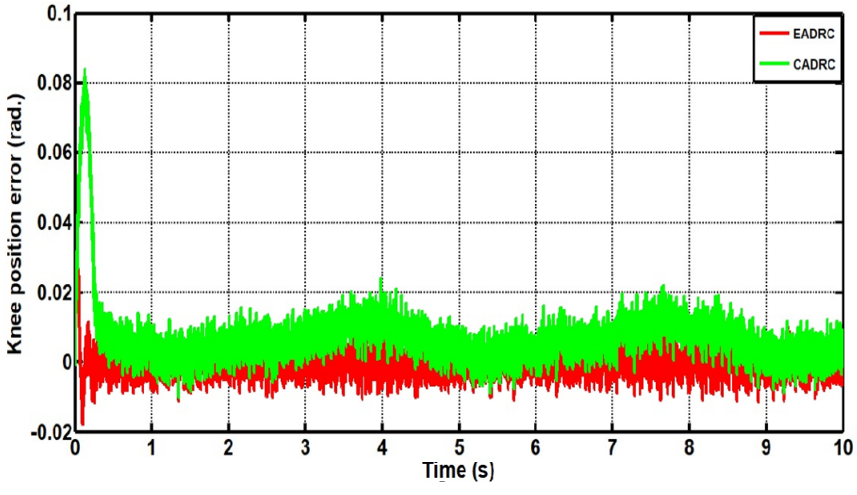

We plot extra state $Z_3(t)$ vs. its aim to assess the ESO's performance (total disturbances). Disturbances are depicted in Figure 10. For EADRC, estimate $Z_3(t)$ shows a strong correlation with total disturbances.

Figure 9 Control torque required for comparison between EADRC and CADRC with noise disturbance (see online version for colours)

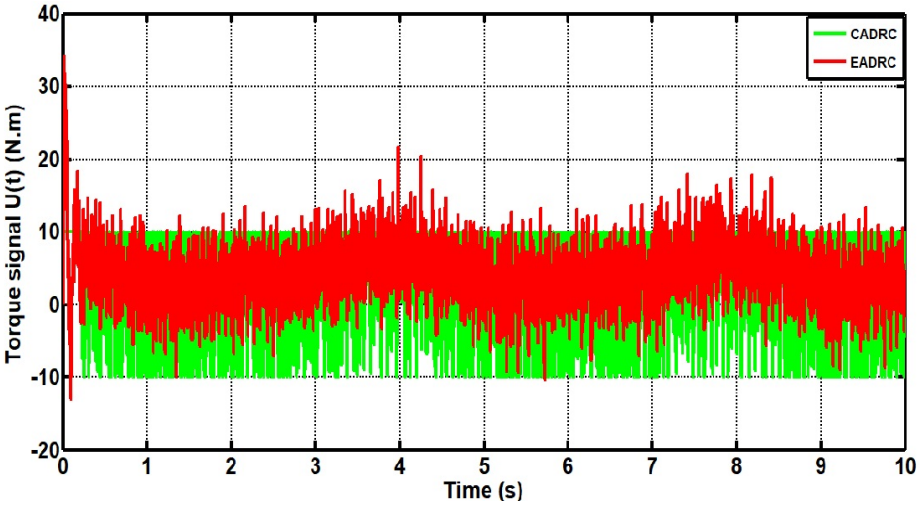

Figure 10 Total disturbances and its estimation for EDRC with noise disturbance (see online version for colours)

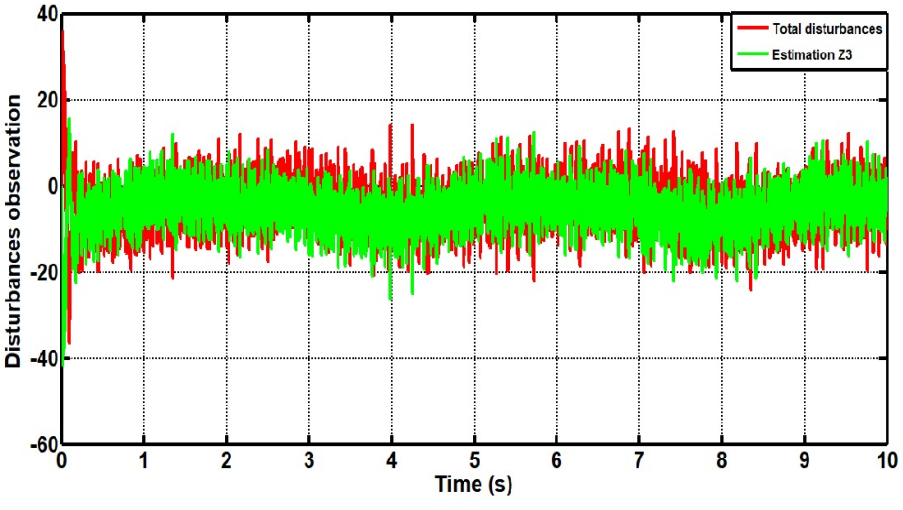

Case 3 with uncertainty effect

It was assumed in the simulation performed up to this point in this section that a second-order nonlinear model could reasonably demonstrate the present situation. In the real world, such a model is generally often the result of ignoring certain dynamical changes, such as inertia and friction. To demonstrate this behaviour, consider how to handle the uncertainty in the model's equation (7) caused by variations in the inertia (J) or frictional effects. Assuming the inertia (J) in this work is changed by ±50% from nominal value. Figure 11 shows trajectory tracking performance allows us to evaluate the EADRC controller's effectiveness while taking uncertainty into consideration, where all

position responses seem to match the expected trajectory. Figure 12 shows the difference in knee angles between the desired and actual positions. The EADRC control technique achieves acceptable tracking error with different uncertainty, demonstrating its usefulness and superiority. Figure 13 depicts the control efforts required to study the required control torque (τ_e) or $u(t)$ with different uncertainty. When compared to Nominal case, the EADRC control method for(–50%)uncertainty yields the shortest control effort required for a controller (ISU) and the smallest RMSE, but with high measure of chattering reduction in control signal index (IAU), as shown in Table 4. It seen that the EADRC method for high uncertainty (+50%) represents the worst case.

Figure 11 Time response comparison of EADRC with different uncertainty (see online version for colours)

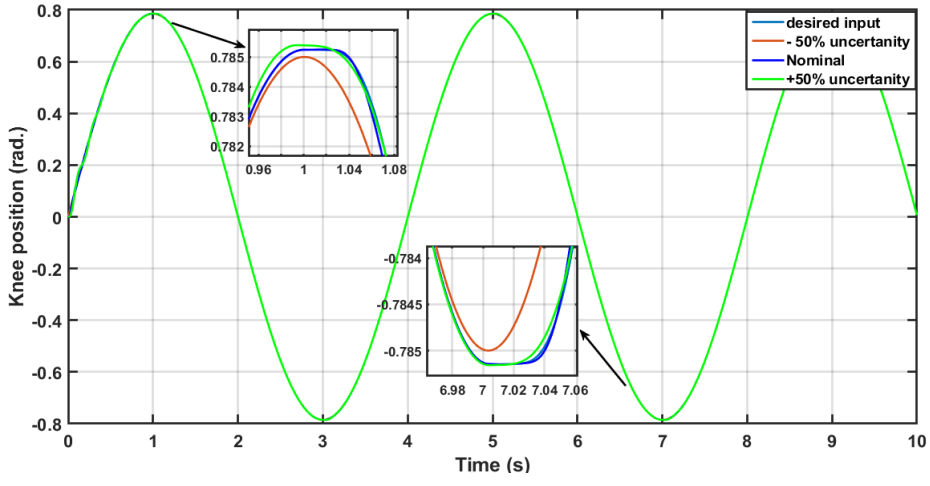

Figure 12 Tracking error comparison of EADRC with different uncertainty (see online version for colours)

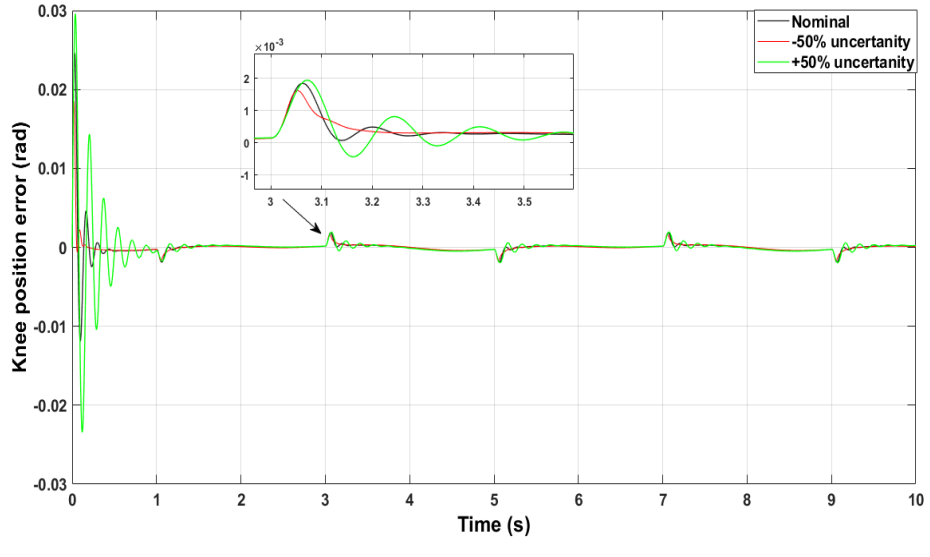

Figure 13 Control torque required of EADRC with different uncertainty (see online version for colours)

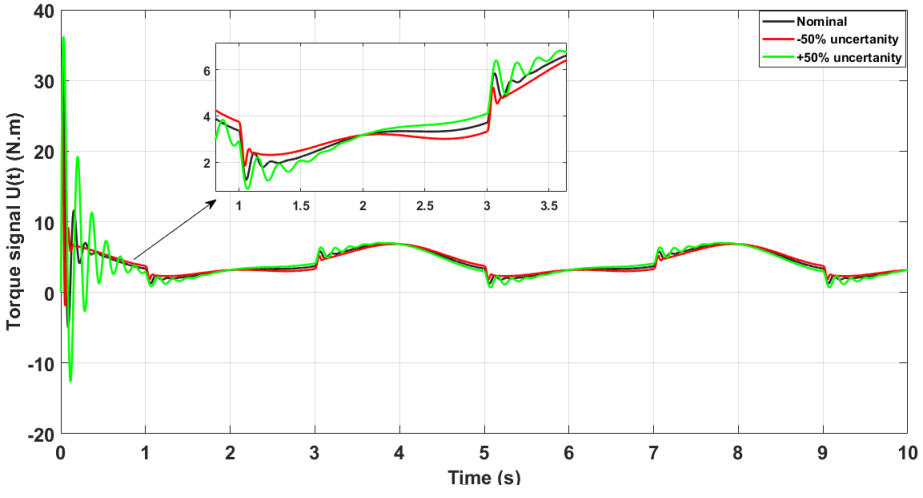

Table 4 Performance indices for EADRC with different uncertainty

EADRC method	*RMSE* (rad.)	*IAE* (rad.)	*ISE* (rad.)	*ISU* (N.m)	*IAU* (N.m)
Nominal case	0.0016	0.0042	$2.67*10^{-5}$	229	24.36
–50% uncertainty	0.0009	0.0029	$9.05*10^{-6}$	212.9	42.38
+50% uncertainty	0.0028	0.0077	$7.6*10^{-5}$	270.1	43.07

Other control strategies might be suggested in order to expand on the current work in the future, to improve the ADRC or to compare performance (Nasir et al., 2022, 2023c, 2023d; Jaydeep, 2022; Pooyan et al., 2022; Leonardo et al., 2019; Sajid et al., 2020).

6 Conclusion

In this study, trajectory tracking control for knee-joint motion has been presented for rehabilitation service using exoskeleton device. An active disturbance rejection control using error-based state-feedback observer has been designed. The effectiveness of EADRC approach has been demonstrated via numerical simulation. A comparison study has been made between the proposed ADRC and the conventional ADRC. The numerical results showed that the proposed controller has better tracking errors and higher noise and load rejection capabilities as compared to conventional ADRC. In addition, the EADRC has simple design and could avoid the use of derivative signals; which is a prerequisite in most conventional ADRC structures.

References

Abdul-Adheem, W.R., Ibraheem, I.K., Humaidi, A.J. and Azar, A.T. (2021) 'Model-free active input–output feedback linearization of a single-link flexible joint manipulator: an improved active disturbance rejection control approach', *Measurement and Control*, Vol. 54, Nos. 5–6, pp.856–871.

Chen, X., Li, D., Gao, Z. and Wang, C. (2011) 'Tuning method for second-order active disturbance rejection control', *Proceedings of the 30th Chinese Control Conference*, 22–24 July, Yantai, China, pp.6322–6327.

Christopher, C., Weiguang, H., Enrico, F., Samer, M., Will, H. and Ravi, V. (2021) 'Model predictive control for human-centred lower limb robotic assistance', *IEEE Transactions on Medical Robotics and Bionics*, Vol. 3, No. 4, pp.1–12.

Congzhi, H., Bin, D. and Chaomin, L. (2020) 'Performance optimisation of discrete time linear active disturbance rejection control approach', *International Journal of Automation and Control*, Vol. 14, Nos. 5–6, pp.713–733.

Dariusz, P., Radosiaw, P., Bartiomiej, K. and Krzysztof, K. (2020) 'Analysis of an impact of inertia parameter in active disturbance rejection control structures', *Electronics*, Vol. 9, pp.1–13.

Domingos, L.A., André, F.O., Túlio, F., de., Junio, A., de. and Edgard, M. (2021) 'Comparison of controller's performance for a knee joint model based on functional electrical stimulation input', *International IEEE/EMBS Conference on Neural Engineering (NER) Virtual Conference*, 4–6 May, Italy, pp.836–839.

Gallagher, J.F., Sivan, M. and Levesley, M. (2022) 'Making best use of home-based rehabilitation robots', *Applied Sciences*, Vol. 12, pp.1–15.

Gao, Z. (2014) 'On the centrality of disturbance rejection in automatic control', *ISA Transactions*, Vol. 53, No. 4, pp.850–857.

Gernot, H. (2013) 'A simulative study on active disturbance rejection control (ADRC) as a control tool for practitioners', *Electronics*, Vol. 2, pp.246–279.

Han, J. (2008) 'From PID to active disturbance rejection control', *IEEE Trans. Ind. Electron.*, Vol. 56, pp.900–906.

Humaidi, A.J. and Badr, H.M. (2018a) 'Linear and nonlinear active disturbance rejection controllers for single-link flexible joint robot manipulator based on PSO tuner', *Journal of Engineering Science and Technology Review*, Vol. 11, No. 3, pp.133–138.

Humaidi, A.J., Badr, H.M. and Ajil, A.R. (2018b) 'Design of active disturbance rejection control for single-link flexible joint robot manipulator', *22nd International Conference on System Theory, Control and Computing*, 10–12 October, Sinaia, Romania, pp.452–457.

Jaydeep, S. (2022) 'Implementation of discrete-time fractional-order derivative controller for a class of double integrating system', *International Journal of Automation and Control*, Vol. 16, No. 2, pp.183–204.

Leonardo, G., Oscar, C., Andrés, R. and Javier, G. (2019) 'A linear algebra controller based on reduced order models applied to trajectory tracking for mobile robots: an experimental validation', *International Journal of Automation and Control*, Vol. 13, No. 2, pp.176–196.

Madonski, R., Ramirez-Neria, M., Stankovic, M., Shao, S., Gao, Z., Yang, J. and Li, S. (2019b) 'On vibration suppression and trajectory tracking in largely uncertain torsional system: an error-based ADRC approach', *Mechanical Systems and Signal Processing*, Vol. 134, pp.1–21.

Madonski, R., Shao, S., Zhang, H., Gao, Z., Yang, J. and Li, S. (2019a) 'General error-based active disturbance rejection control for swift industrial implementations', *Control. Eng. Pract.*, Vol. 84, pp.218–229.

Michael, M.M. (2016) 'Robust trajectory following without availability of the reference time-derivatives in the control scheme with active disturbance rejection', *Proceedings of the 2016 American Control Conference* (*ACC*), 6–8 July, Boston, MA, USA, pp.1536–1541.

Nasir, A.A., Amjad, J.H. and Ahmed, S.A. (2022) 'Observer sliding mode control design for lower exoskeleton system: rehabilitation case', *Journal of Robotics and Control*, Vol. 3, No. 4, pp.476–482.

Nasir, A.A., Amjad, J.H. and Ahmed, S.A. (2023a) 'Sliding mode-based active disturbance rejection control of assistive exoskeleton device for rehabilitation of disabled lower limbs', *An Acad Bras Cienc*, Vol. 95, No. 2, pp.1–17.

Nasir, A.A., Amjad, J.H. and Ahmed, S.A. (2023b) 'A novel approach of multi-loop control based ADRC for improving lower knee position exoskeleton system', *International Review of Applied Sciences and Engineering*, Vol. 14, No. 3, pp.316–324.

Nasir, A.A., Amjad, J.H. and Ahmed, S.A. (2023c) 'Active disturbance rejection control with decoupling case for a lower limb exoskeleton of swing leg', *ICIC Express Letters*, Vol. 17, No. 11, pp.1263–1275.

Nasir, A.A., Amjad, J.H. and Ahmed, S.A. (2023d) 'Fractional multi-loop active disturbance rejection control for a lower knee exoskeleton system', *Acta Polytechnica*, Vol. 63, No. 3, pp.158–170.

Pooyan, A.H., Ali, S.S. and Saad, M. (2022) 'Fuzzy adaptive finite-time sliding mode controller for trajectory tracking of ship course systems with mismatched uncertainties', *International Journal of Automation and Control*, Vol. 16, Nos. 3–4, pp.255–271.

Radosiaw, P. and Dariusz, P. (2021) 'Improving the active disturbance rejection controller tracking quality by the input-gain underestimation for a second-order plant', *Electronics*, Vol. 10, No. 8, pp.1–16.

Ramirez-Neria, M., Madonski, R., Luviano-Juarez, A., Gao, Z. and Sira-Ramirez, H. (2020) 'Design of ADRC for second-order mechanical systems without time-derivatives in the tracking controller', *Proceedings of the American Control Conference*, 1–3 July, Denver, CO, USA, pp.2623–2628.

Saber, M. and Djamel, E.C. (2019) 'A robust control scheme based on sliding mode observer to drive a knee-exoskeleton', *Asian Journal of Control*, Vol. 21, No. 1, pp.439–455.

Sajid, R.A., Poovaneswaran, P.M.S., Hossain Lipu, M.A.H. and Pin, J.K. (2020) 'A comparative evaluation of PID-based optimisation controller algorithms for DC motor', *International Journal of Automation and Control*, Vol. 14, Nos. 5–6, pp.634–655.

Song, K., Upadhyay, D. and Xie, H. (2019) 'Control of diesel engines with electrically assisted turbocharging through an extended state observer based nonlinear MPC', *Proc IMechE, Part D: J. Automobile Engineering*, Vol. 233, No. 2, pp.378–395.

Tian, G. and Gao, Z. (2009) 'Benchmark tests of active disturbance rejection control on an industrial motion control platform', *2009American Control Conference*, 10–12 June, St. Louis, MO, USA, pp.5552–5557.

Venkatesh, M., Sourav, P. and Goshaidas, R. (2021) 'Observer-based controller design for linear time-varying delay systems using a new Lyapunov-Krasovskii functional', *International Journal of Automation and Control*, Vol. 15, No. 1, pp.99–123.

Vivek, P., Dipayan, G. and Shubhi, P. (2023) 'Disturbance observer-based higher-order sliding mode controller for frequency regulation of hybrid power systems', *International Journal of Automation and Control*, Vol. 17, No. 2, pp.188–226.

Wameedh, R.A., Ibraheem, K.I. and Amjad, J.H. (2020) 'Novel active disturbance rejection control based on nested linear extended state observers', *Appl. Sci*., Vol. 10, pp.1–27.

Zhao, S. and Gao, Z. (2010) 'An active disturbance rejection based approach to vibration suppression in two-inertia systems', *Proceedings of the 2010 American Control Conference,* 30 June–02 July, Baltimore, MD, USA, pp.1520–1525.

Zheng, Q., Chen, Z. and Gao, Z. (2009) 'A practical dynamic decoupling control approach', *Control Engineering Practice*, Vol. 17, pp.1016–1025.

Zheng, Q., Dong, L. and Gao, Z. (2007) 'A novel control system design for vibrational MEMS gyroscopes', *Sensors and Transducers Journal*, Vol. 78, No. 4, pp.1073–1082.